

Review

# Probing the Bioinorganic Chemistry of Cu(I) with $^{111}\text{Ag}$ Perturbed Angular Correlation (PAC) Spectroscopy

Victoria Karner <sup>1</sup>, Attila Jancso <sup>2</sup>  and Lars Hemmingsen <sup>3,\*</sup> <sup>1</sup> TRIUMF, 4004 Wesbrook Mall, Vancouver, BC V6T 2A3, Canada; vkarner@triumf.ca<sup>2</sup> Department of Molecular and Analytical Chemistry, University of Szeged, Dóm tér 7-8, H-6720 Szeged, Hungary; jancso@chem.u-szeged.hu<sup>3</sup> Department of Chemistry, University of Copenhagen, Universitetsparken 5, DK-2100 Copenhagen, Denmark

\* Correspondence: lhe@chem.ku.dk

**Abstract:** The two most common oxidation states of copper in biochemistry are Cu(II) and Cu(I), and while Cu(II) lends itself to spectroscopic interrogation, Cu(I) is silent in most techniques. Ag(I) and Cu(I) are both closed-shell  $d^{10}$  monovalent ions, and to some extent share ligand and coordination geometry preferences. Therefore, Ag(I) may be applied to explore Cu(I) binding sites in biomolecules. Here, we review applications of  $^{111}\text{Ag}$  perturbed angular correlation (PAC) of  $\gamma$ -ray spectroscopy aimed to elucidate the chemistry of Cu(I) in biological systems. Examples span from small blue copper proteins such as plastocyanin and azurin (electron transport) over hemocyanin (oxygen transport) to CueR and BxmR (metal-ion-sensing proteins). Finally, possible future applications are discussed.  $^{111}\text{Ag}$  is a radionuclide which undergoes  $\beta$ -decay to  $^{111}\text{Cd}$ , and it is a  $\gamma$ - $\gamma$  cascade of the  $^{111}\text{Cd}$  daughter nucleus, which is used in PAC measurements.  $^{111}\text{Ag}$  PAC spectroscopy may provide information on the coordination environment of Ag(I) and on the structural relaxation occurring upon the essentially instantaneous change from Ag(I) to Cd(II).

**Keywords:** copper proteins; copper biochemistry; Cu(I); spectroscopy; metal site structure and rigidity; Ag(I) binding to proteins



**Citation:** Karner, V.; Jancso, A.; Hemmingsen, L. Probing the Bioinorganic Chemistry of Cu(I) with  $^{111}\text{Ag}$  Perturbed Angular Correlation (PAC) Spectroscopy. *Inorganics* **2023**, *11*, 375. <https://doi.org/10.3390/inorganics11100375>

Academic Editors: Christelle Hureau, Ana Maria Da Costa Ferreira and Gianella Facchin

Received: 28 August 2023

Revised: 18 September 2023

Accepted: 19 September 2023

Published: 23 September 2023



**Copyright:** © 2023 by the authors. Licensee MDPI, Basel, Switzerland. This article is an open access article distributed under the terms and conditions of the Creative Commons Attribution (CC BY) license (<https://creativecommons.org/licenses/by/4.0/>).

## 1. Introduction

Copper ions take part in fundamental biochemical processes such as electron transfer, oxygen transport, enzyme catalyzed redox reactions, and systems to control copper itself in the cell (transcriptional regulators, chaperones, and transmembrane transporters) [1–4]. The most common oxidation states are Cu(I) and Cu(II), and while Cu(II) is observable by several experimental methods, Cu(I) is a closed-shell ( $d^{10}$ ) ion and therefore silent in most spectroscopic techniques, except nuclear and X-ray based approaches such as EXAFS, XANES, NMR/NQR, and potentially  $\beta$ -NMR [5,6]. Similarly, other closed-shell ions such as Mg(II), Ca(II), and Zn(II) pose a challenge in terms of the spectroscopic characterization of their coordination environments. Substitution of spectroscopically silent native metal ions by active probes such as Co(II), Mn(II), and  $^{113}\text{Cd}$ (II) (for NMR) has found widespread use in the characterization of the metal site structure and function of metalloproteins [7,8]. Similarly, Ag(I) has been used in a number of studies to explore copper biochemistry [9–17], despite the fact that Ag(I) in itself is also silent in most spectroscopic analyses.

In perturbed angular correlation (PAC) of  $\gamma$ -ray spectroscopy,  $^{111m}\text{Cd}$  has been employed as a means to probe the function of several Zn-dependent enzymes [18], and in the context of this minireview, the less commonly used  $^{111}\text{Ag}$  is of particular interest to explore the biochemistry of Cu(I) and potentially in radiopharmaceutical applications [19,20]. As a group 11 element, Ag is a heavier congener of Cu, and not surprisingly Ag(I) and Cu(I) exhibit common properties such as coordination with soft ligands, most notably thiolates in proteins, and geometries of metal sites, although the ionic radius of Ag(I) is larger than that of Cu(I).  $^{111}\text{Ag}$  PAC spectroscopy has been applied in a limited number of (bio)inorganic

chemistry studies so far, including small inorganic compounds [21–23], Ag(I) chelators with potential radiopharmaceutical applications [19,20], and metalloproteins. One of the key advantages of PAC spectroscopy is that it relies on a radioactive probe; and so akin to radiotracer techniques, only very small amounts of the probe are required to record a spectrum, typically on the order of picomoles (or  $10^{11}$  probe ions or atoms) [18]. Moreover, PAC spectroscopy may be applied to any physical state (solid, liquid, or gas) [18,24], and as most biological material is transparent to  $\gamma$ -rays, even in vivo PAC experiments are possible [25].  $^{111}\text{Ag}$  may be produced at radioactive ion beam facilities such as ISOLDE/CERN or by neutron irradiation of isotopically enriched  $^{110}\text{Pd}$  at facilities such as ILL, Grenoble, France. The relatively long half-life ( $T_{1/2} = 7.45$  days) allows for shipping from a production facility to the home lab, and as such, makes  $^{111}\text{Ag}$  an attractive PAC probe.

With this work, we review applications of  $^{111}\text{Ag}$  PAC spectroscopy within Cu(I) bioinorganic chemistry, which so far only encompasses electron transfer proteins (plastocyanin and azurin) [26–29], an oxygen transport protein (hemocyanin) [30], and metal-ion-sensing proteins functioning as transcriptional regulators (CueR and BxmR) [31–33].

## 2. PAC Theory

In this section, we provide a brief introduction to PAC spectroscopy with an emphasis on  $^{111}\text{Ag}$  PAC; for a more detailed analysis of the technique, we refer the reader to [18].

In PAC spectroscopy, the hyperfine interactions between the nuclear magnetic and/or quadrupole moments of the probe nucleus and the local magnetic fields and/or electric field gradients (EFGs) are measured through the perturbed angular correlation of a  $\gamma$ - $\gamma$  cascade in the nuclear decay. In this review, we will focus solely on interactions between the nuclear quadrupole moment of the PAC nucleus and the EFG of its surroundings, i.e., the nuclear quadrupole interaction (NQI). An EFG is a signature of the local electronic and molecular structure surrounding the PAC probe site, and if the EFG is time-dependent, dynamics may also be explored typically on the ps–ns time scale. The NQI gives rise to hyperfine splitting of the nuclear energy levels of the probe nucleus, and this energy splitting is measured via PAC spectroscopy for the intermediate level of the  $\gamma$ - $\gamma$  cascade. For a nucleus with spin  $I = 5/2$ , such as the relevant nuclear level of many PAC probes including  $^{111}\text{Ag}$ , the intermediate energy level is split into three sublevels with transition frequencies of  $\omega_1$ ,  $\omega_2$ , and  $\omega_3$  between these sublevels. Note that this invokes the rule that  $\omega_3 = \omega_1 + \omega_2$ . These frequencies serve as a fingerprint for the local structure at the probe site.

For randomly oriented molecules and a time-independent NQI, the measured data reflect the so-called perturbation function, which, for  $I = 5/2$ , is given by:

$$G_2(t) = a_0 + a_1 \cos(\omega_1 t) + a_2 \cos(\omega_2 t) + a_3 \cos(\omega_3 t) \quad (1)$$

where  $a_i$  and  $\omega_i$  depend on only two parameters, the NQI strength typically reported as  $\nu_Q$  or  $\omega_0$ , which is proportional to  $|V_{zz}|$ , and the axial asymmetry parameter  $\eta = (V_{yy} - V_{xx})/V_{zz}$ , where  $V_{xx}$ ,  $V_{yy}$ , and  $V_{zz}$  are the diagonal elements of the EFG tensor in the principal axis system, ordered such that  $|V_{zz}| \geq |V_{yy}| \geq |V_{xx}|$ .

Figure 1 shows the decay schemes of  $^{111}\text{Ag}$  and  $^{111\text{m}}\text{Cd}$ . Note that  $^{111}\text{Ag}$  does not directly undergo the necessary  $\gamma$ - $\gamma$  cascade for PAC spectroscopy, instead it decays by  $\beta^-$  emission to  $^{111}\text{Cd}$ , and with a  $\sim 7\%$  chance, the “correct” excited state of  $^{111}\text{Cd}$  is populated (342 keV) which then may decay by the successive emission of two  $\gamma$ -rays necessary for PAC. The intermediate level probed in this cascade has a half-life of 85 ns, and it is the NQI that the Cd nucleus experiences in this state which is measured in  $^{111}\text{Ag}$  PAC experiments.

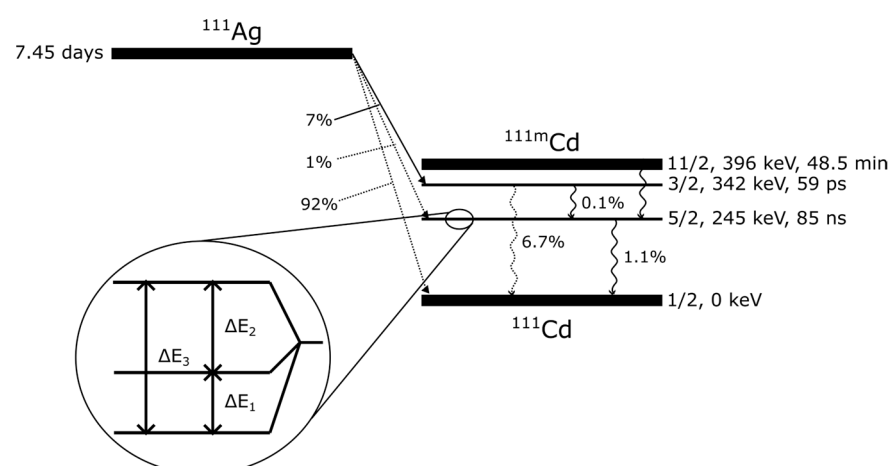


**Figure 1.** Nuclear decay of  $^{111}\text{Ag}$ . The probabilities of the various decay routes are given per  $^{111}\text{Ag}$  decay. The decay of  $^{111\text{m}}\text{Cd}$  (another commonly used PAC isotope) is also indicated to demonstrate that the hyperfine splitting of the same intermediate level ( $I = 5/2$ , 245 keV) is probed in  $\gamma$ - $\gamma$  PAC spectroscopy in the two radionuclides, although the first  $\gamma$  differs for the  $\gamma$ - $\gamma$  cascade in  $^{111}\text{Ag}$  PAC and  $^{111\text{m}}\text{Cd}$  PAC.

If the EFG is time-dependent on the ps–ns time scale, the perturbation function, Equation (1), is affected. If the motion is slow ( $1/\tau_c \ll \omega_0$ ), the perturbation function is exponentially dampened by  $\exp(-t/\tau_c)$ , where  $\tau_c$  is the characteristic time of the (stochastic) dynamics, for example, the rotational correlation time of a molecule undergoing rotational diffusion. If the motion is fast ( $1/\tau_c \gg \omega_0$ ), the perturbation function becomes  $G_2(t) = \exp(-2.8\omega_0^2\tau_c(1 + \eta^2/3)t)$ , i.e., a purely exponentially decaying function. If the dynamics originate from chemical exchange between two (or more) species, three different scenarios are possible, in analogy to NMR spectroscopy: slow exchange where both species are observed, intermediate exchange where line broadening is pronounced, and fast exchange where a weighted average signal is observed.

### 3. Examples of Applications of $^{111}\text{Ag}$ PAC Spectroscopy Elucidating Cu(I) Bioinorganic Chemistry

In this section, we aim to provide an overview of the type of questions which can be addressed with  $^{111}\text{Ag}$  PAC spectroscopy. We begin with a series of literature examples, and we end with suggestions for future applications of the technique.

#### 3.1. Metal Site Structure in Small Blue Copper Proteins—Electron Transport and Transfer

Small blue copper proteins take part in the transport of electrons. The prototypical example is plastocyanin, transporting electrons in photosynthesis from cytochrome  $b_6/f$ , diffusing as Cu(I)-plastocyanin to associate with and transfer the electron to photosystem I. The metal site is composed of two histidine residues and one cysteine residue in a distorted trigonal planar structure, with an additional methionine residue at an axial position and with an unusual distance from the metal ion to the thioether sulfur of around 3 Å, see Figure 2. The metal site is assumed to be rigid, and crystallographic data indicate that there is very little difference in the Cu(I) and Cu(II) coordination geometry [34], presumably facilitating rapid electron transfer. In a broader perspective, these so-called type I copper sites are an important class of Cu-binding sites which are present in many copper-containing proteins, most notably in blue multicopper oxidases.

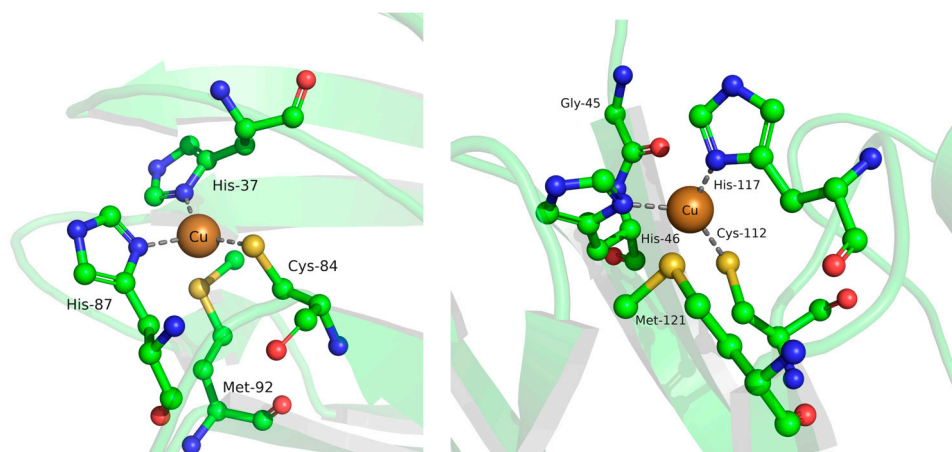


**Figure 2.** Metal sites of plastocyanin (left) and azurin (right). A copper ion is bound in a distorted trigonal planar structure with two His residues, one Cys residue, and an axial Met residue at an uncommon distance of ca. 3 Å from the metal ion (pdb codes: 1PLC [35] and 1AZC [36]). Figure produced with PyMOL [37].

$^{111}\text{Ag}$  and  $^{111\text{m}}\text{Cd}$  PAC was employed to determine if there is a difference between the metal site structure of the monovalent Ag(I) and the divalent Cd(II)-substituted azurin, or if the protein fully dictates the metal site structure [26]. The PAC spectra are presented in Figure 3, demonstrating that there is very little difference between the recorded NQIs for  $^{111}\text{Ag}$ (I) azurin and  $^{111\text{m}}\text{Cd}$ (II) wild-type (WT) azurin (lower panel). The small (but statistically significant) difference may be accounted for by changes in the ligand–metal–ligand angles of a few degrees [26]. Interestingly, the (small) difference between the NQIs from  $^{111}\text{Ag}$  and  $^{111\text{m}}\text{Cd}$  PAC is most pronounced in the  $^{111}\text{Ag}$  PAC data for the first ca. 60 ns after the decay from  $^{111}\text{Ag}$  to  $^{111}\text{Cd}$ , while at longer times (60–120 ns) after the decay, the NQI approaches the value recorded by  $^{111\text{m}}\text{Cd}$  PAC. This indicates that although the structures of Ag(I) and Cd(II) are highly similar, (minor) structural relaxation occurs on the nanosecond time scale upon the decay of  $^{111}\text{Ag}$  to  $^{111}\text{Cd}$ . This model was corroborated by PAC experiments at two different temperatures (1 °C and 25 °C), demonstrating that the rate of relaxation increased by around a factor of 2 when increasing the temperature from 1 to 25 °C. Thus,  $^{111}\text{Ag}$  PAC spectroscopy allowed for an estimate of the rate of the (small) structural reorganization occurring when the metal ion changed from monovalent Ag(I) to divalent Cd(II), in analogy to a pump–probe experiment, where the “pump” is the nuclear decay of  $^{111}\text{Ag}$ , and the probing is performed by following the time-dependent change in the metal site NQI.

Mutation of the methionine near the metal site to leucine, forming M121L azurin, is a way to probe if M121 significantly affects the metal site structure. Interestingly,  $^{111}\text{Ag}$  PAC spectra of the M121L mutant show very little change compared to the WT protein, see Figure 3, top panel, while the  $^{111\text{m}}\text{Cd}$  PAC spectra exhibit one NQI similar to the WT signal, but another NQI (with significant line broadening, reflecting structural variability) also appears. Thus, it seems that the introduction of both a mutation (M121L) and a non-native metal ion with different combination of electronic structure ( $d^{10}$ ) and charge (Cd(II)) from Cu(I) and Cu(II) leaves the metal site less well defined. Similarly,  $^{111}\text{Ag}$  PAC spectra of the M121H mutant of azurin [27] gave rise to significantly more diverse coordination geometries than observed for the WT protein. As a function of pH from 4.0 to 7.7, four different NQIs were observed and interpreted as  $[\text{AgHisCys}(\text{H}_2\text{O})_2]$  at low pH, and three different  $[\text{AgHis}_2\text{Cys}(\text{H}_2\text{O})]$  structures in various proportions at the higher pH values, where the changes are controlled by the protonation states of the histidine residues. Thus, M121H mutation significantly alters the metal site properties.

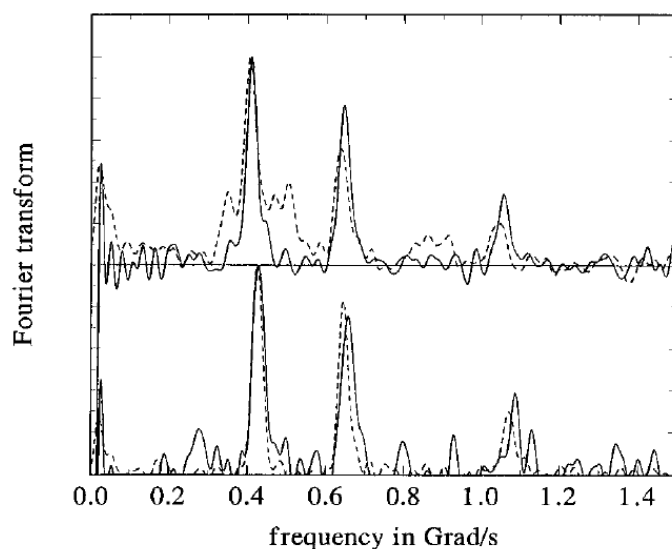


**Figure 3.**  $^{111}\text{Ag}$  and  $^{111\text{m}}\text{Cd}$  PAC spectra of azurin and M121L azurin. Lower panel:  $^{111}\text{Ag}$  PAC spectrum (solid line) and  $^{111\text{m}}\text{Cd}$  PAC spectrum (dotted line) for wild-type azurin. Upper panel:  $^{111}\text{Ag}$  PAC spectrum (solid line) and  $^{111\text{m}}\text{Cd}$  PAC spectrum (dotted line) for M121L azurin. The Fourier transform for  $^{111}\text{Ag}$  PAC is multiplied by  $-1$  for easy comparison with the Fourier transform for  $^{111\text{m}}\text{Cd}$  PAC. Reprinted with permission from Ref. [26]. Copyright American Chemical Society 1997.

### 3.2. Plastocyanin–Photosystem I Association—Protein–Protein Interactions in Electron Transport

Reduced photosystem I is the physiological partner to which Cu(I)-plastocyanin transfers an electron. In analogy to the study of azurin, *vide supra*,  $^{111}\text{Ag}$  and  $^{111\text{m}}\text{Cd}$  PAC spectra were recorded for Ag(I)- and Cd(II)-substituted plastocyanin, and the measured NQIs were very similar, indicating that Ag(I) and Cd(II) occupy very similar metal site structures [28] with distorted trigonal planar coordination by two histidine residues and one cysteine residue. In a pH series from 5.0 to 8.5, the low pH spectra indicated significant changes in the first coordination sphere, presumably reflecting dissociation of one of the His residues and coordination by the axial methionine thioether [29], in agreement with data obtained by X-ray diffraction at low pH [38]. The main point of the current subsection is, however, that it is possible to monitor the binding of Ag(I)-plastocyanin and Cd(II)-plastocyanin to reduced photosystem I, see Figure 4 [28]. In the absence of photosystem I (top panels of Figure 4), both the  $^{111}\text{Ag}$ (I)-plastocyanin and the  $^{111\text{m}}\text{Cd}$ (II)-plastocyanin data display heavy damping of the oscillatory signal; this is caused by rotational diffusion of the protein, which is relatively rapid under the experimental conditions. However, upon addition of photosystem I, the oscillations of the observed perturbation function for  $^{111}\text{Ag}$ -plastocyanin are recovered, indicating that the Brownian tumbling of the protein is much slower, i.e., that  $^{111}\text{Ag}$ -plastocyanin is bound to photosystem I. Contrary to this, no indication of binding of  $^{111\text{m}}\text{Cd}$ -plastocyanin to photosystem I is observed, in accordance with the function of plastocyanin. Moreover, the binding of  $^{111}\text{Ag}$ -plastocyanin to photosystem I eliminates the relaxation of the  $^{111}\text{Ag}$  metal site structure to that observed for  $^{111\text{m}}\text{Cd}$ , implying that the metal site structure and association with photosystem are mutually affecting each other.

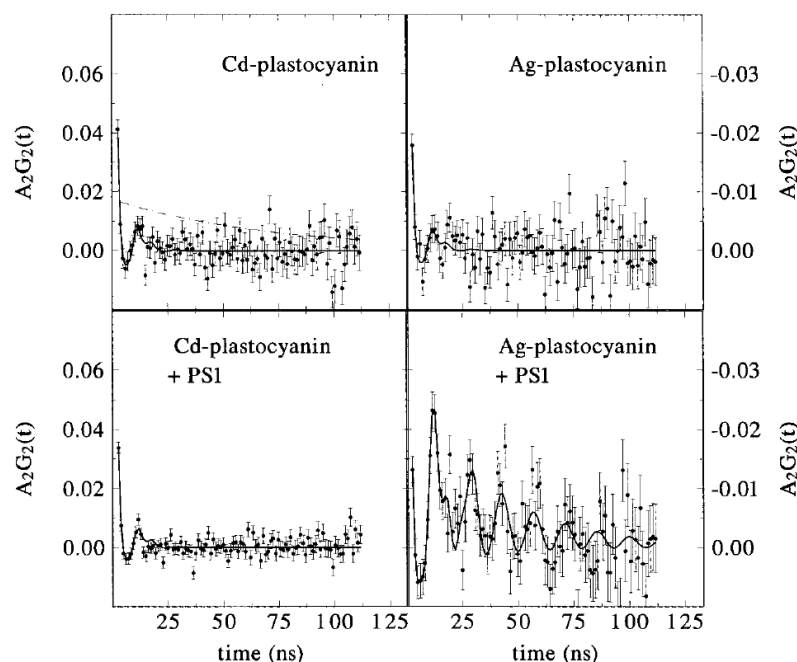


**Figure 4.**  $^{111}\text{Ag}$ - and  $^{111\text{m}}\text{Cd}$  PAC time traces recorded for plastocyanin in the absence and presence of photosystem I. Left panels:  $^{111\text{m}}\text{Cd}$  PAC data for plastocyanin in the absence (top) and presence (bottom) of photosystem I. Right panels:  $^{111}\text{Ag}$  PAC data for plastocyanin in the absence (top) and presence (bottom) of photosystem I. Data points indicated with error bars, and fit (solid lines) using Equation (1) with exponential damping due to rotational diffusion. The data for  $^{111}\text{Ag}$  PAC are multiplied by  $-1$  for easy comparison with the  $^{111\text{m}}\text{Cd}$  PAC data. Reprinted with permission from ref. [28]. Copyright American Chemical Society 1999.

### 3.3. Metal Site Structure in Hemocyanin—Oxygen Transport

Hemocyanins (Hcs) transport oxygen in the hemolymph of some mollusks and arthropods. The oxygen binding site is composed of two copper ions coordinated by three histidine residues each, see Figure 5. In the absence of oxygen, both metal ions are reduced, while upon oxygen binding, they are oxidized to Cu(II) and accordingly oxygen is reduced to the peroxide ion.

The binuclear Cu site in deoxy-Hc from the arthropod *Carcinus aestuarii* was characterized by  $^{111}\text{Ag}$  PAC spectroscopy by Holm et al. [30] through a series of experiments with varying Ag(I)-to-protein ratios. Note that the amount of radioactive  $^{111}\text{Ag}$  is very small, so the Ag(I) concentration is controlled by the addition of non-radioactive Ag(I), typically as a nitrate or perchlorate salt. With 0.1 eq. Ag(I) with respect to 0.5 mM Hc, a PAC signal with  $\omega_0 = 0.183(1)$  rad/ns and  $\eta = 0.18(3)$  was observed. Increasing the Ag(I) concentration to 2.0 eq. Ag(I) gave rise to a different signal with a larger line width (i.e., increased width in the distribution of NQIs) and an increase in the asymmetry parameter to  $\eta = 0.26(4)$ , if fitting the data with only one NQI. Although these changes are small, they are statistically significant, and in particular, the increased line width is qualitatively observable in the data. Fitting the 2.0 eq. Ag(I) data with two NQIs instead gives roughly equal amplitudes for the two signals, as expected for full occupation of the two metal sites in Hc. The PAC parameters differ (for both sites) from those observed at 0.1 eq. Ag(I). Thus, it was concluded that the protein displays two slightly different metal ion binding sites, and that the NQI recorded for site 1 depends on whether site 2 is occupied or not, indicating that they are close in space, in agreement with the structure, see Figure 5. An additional experiment was carried out with 1.0 eq. Ag(I), and the spectrum differed from that recorded with 0.1 eq. Ag(I), indicating that both sites are occupied in a significant fraction of the proteins in the presence of 1.0 eq. Ag(I), and consequently that the binding of the two metal ions is likely to be cooperative.

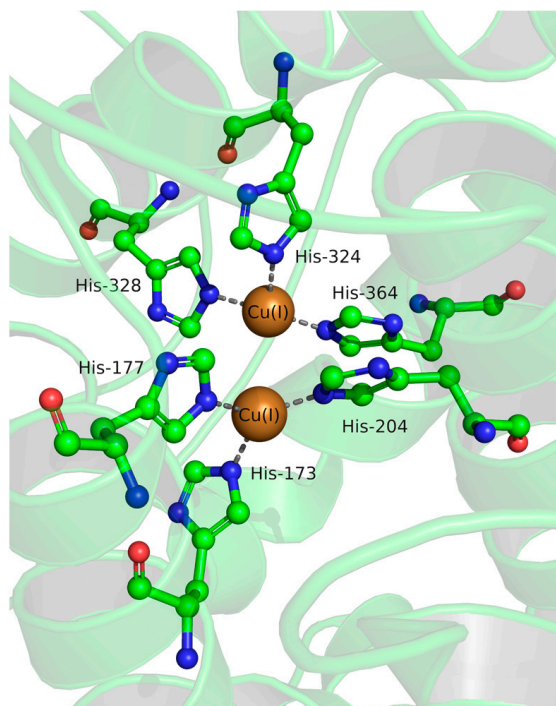


**Figure 5.** Metal site of hemocyanin. In the resting state of the protein (deoxy-Hc), two Cu(I) are present at the dioxygen binding site, each bound by three histidine residues (pdb code: 1LLA [39]). Figure produced with PyMOL [37].

The structural interpretation of the recorded PAC signals was carried out by Holm et al. [30] using the semiempirical angular overlap model (AOM) [40]. It was concluded that purely three-coordinated Ag(I) does not agree well with the  $^{111}\text{Ag}$  PAC spectroscopic data, and that it is likely that a fourth ligand, for example, a water molecule, may be present both with one and with two Ag(I) bound to Hc. In the work by Holm et al. [30], it was assumed that the local Ag(I) metal site structure persisted throughout the PAC measurements, i.e., that little or no structural relaxation occurred, despite the change of element and oxidation state accompanying the nuclear decay of  $^{111}\text{Ag}$ (I) to  $^{111}\text{Cd}$ (II). Later experiments on the CueR transcriptional regulator [32], *vide infra*, have demonstrated that this assumption may not always hold. Therefore, it is conceivable that the conclusion of the analysis of the Hc  $^{111}\text{Ag}$  PAC spectroscopic data should be re-evaluated, and augmented with an additional possibility: (A) the presence of a water molecule bridging the two Ag(I) ions or (B) a water molecule (or another ligand) might be recruited by Cd(II) rapidly after  $^{111}\text{Ag}$  decay. The  $^{111}\text{Ag}$  PAC data reflect the structure(s) present from about 10 to 200 ns after the nuclear decay, which could be long enough for a water molecule to migrate to the metal site. The time scale is controlled by the half-life,  $T_{1/2} = 84$  ns, of the intermediate nuclear level of the  $\gamma$ - $\gamma$  cascade of  $^{111}\text{Cd}$  (because  $T_{1/2}$  of the initial state of the  $\gamma$ - $\gamma$  cascade is much shorter, see Figure 1). Note that the other Ag(I) of the binuclear site will (in almost all cases) be non-radioactive, because only a very small amount of  $^{111}\text{Ag}$  is present with respect to the total amount of added non-radioactive Ag(I). In summary, the experimental data can be interpreted in two different ways: either Ag(I) in Hc from *Carcinus aestuarii* is four-coordinated with a water molecule as the fourth ligand, or Ag(I) is three-coordinated by the three histidine residues, and the fourth ligand is recruited after the decay to Cd(II). To discriminate between these two options, it might be useful to carry out experiments at low temperature, where the chance of trapping Ag(I) in the native coordination environment is higher, *vide infra*.

### 3.4. Metal Site Structure in Cu(I)-Sensing Proteins—Transcriptional Regulation

#### 3.4.1. BxmR

BxmR is a transcriptional regulator protein of the ArsR family with a complex metal ion response profile. Cu(I), Ag(I), and Cd(II) all bind to the so-called  $\alpha$ 3N site in which four cysteine residues are available for metal ion coordination.

$^{111}\text{Ag}$  PAC spectroscopic data display two NQIs, reflecting two different coordination geometries [31].  $^{111\text{m}}\text{Cd}$  PAC spectroscopy, which probes the metal site structure of Cd(II) via the NQIs of the same intermediate nuclear state that is probed in  $^{111}\text{Ag}$  PAC, gives spectra that differ from those of  $^{111}\text{Ag}$  PAC. This indicates that the NQIs observed by  $^{111}\text{Ag}$  PAC are specific for Ag(I) coordination. One of the two NQIs observed by  $^{111}\text{Ag}$  PAC spectroscopy has NQI1:  $\omega_0 = 0.23$  rad/ns and  $\eta = 0.33$ , while the other is more difficult to fit, and can either have NQI2:  $\omega_0 = 0.42$  rad/ns and  $\eta = 0.05$  or NQI2':  $\omega_0 = 0.24$  rad/ns and  $\eta = 1$ . In the same paper, a comprehensive analysis of the Cu(I) binding (including XANES, EXAFS, UV-Vis absorption, and luminescence) indicated that a  $\text{Cu(I)}_2\text{S}_4$  cluster is formed, in which each Cu(I) is tri-coordinated. NQI2 agrees well with a trigonal planar structure for Ag(I). Based on the additional work compiled on  $^{111}\text{Ag}$  PAC since this work was published, and on analysis using AOM [40], we tentatively suggest that NQI1 might reflect a  $\text{Ag(I)}_2\text{S}_4$  cluster in which the bridging thiolates have weaker bonding to Ag(I) (and Cd(II)) than the cysteines used to parameterize the AOM. Both structural interpretations are in accordance with the formation of a  $\text{Ag(I)}_2\text{S}_4$  cluster, although other structures may also underlie the observed NQIs.

#### 3.4.2. CueR

CueR is a transcriptional regulator protein of the MerR family with specificity for monovalent ions of the coinage metals [41]. Cu(I) (and Ag(I) and Au(I)) is found in a near linear structure coordinated by two cysteines, see Figure 6. Ser77 from the other monomer of the protein dimer is positioned close to the metal site.

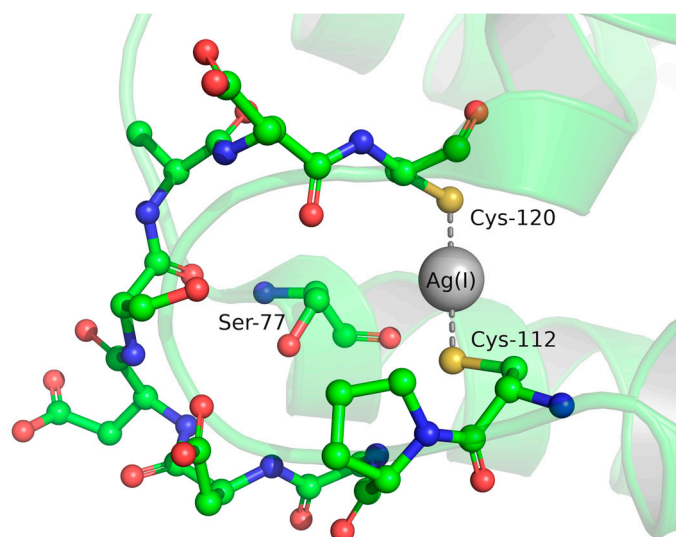


**Figure 6.** Metal site of CueR. Ag(I) is bound in an almost linear structure by two cysteines, and the backbone carbonyl oxygen of Ser77 from the other monomer of the homodimeric protein is located near the metal ion (pdb code: 4WLW [42]). Figure produced with PyMOL [37].

$^{111}\text{Ag}$  PAC was applied to characterize the CueR metal binding site [32,33], see Figure 7, and the decay of  $^{111}\text{Ag}$  to  $^{111}\text{Cd(II)}$  provided a means to elucidate the effect of instantaneously changing from Ag(I), which activates the protein function, to Cd(II), which does not. Contrary to the rigid small blue copper proteins, *vide supra*, significant structural changes are induced at the CueR metal site by the Ag(I) to Cd(II) transition. An experiment conducted at  $-196$  °C displayed two NQIs, reflecting the presence of two

different metal site structures. One of the signals is in good agreement with an almost linear structure with two coordinating thiolates, as expected, possibly with a weak ligand in the equatorial plane, such as carbonyl oxygen, suggested to be from Ser77 (high frequency signal, top panel, Figure 7). The other signal indicated a higher coordination number, thus implying that even at this low temperature, Cd(II) does in some cases recruit more ligands to satisfy this metal ion's preference for coordination numbers higher than two. In a subsequent quantum mechanical molecular dynamics (QM/MD) simulation [43], it was demonstrated that Cd(II) may indeed recruit additional ligands, and probably form a four-coordinate site involving, for example, backbone carbonyl oxygens, in addition to maintaining coordination with the two Cys residues. Interestingly, a  $^{111}\text{Ag}$  PAC experiment at 1 °C exclusively displayed this second signal, demonstrating that the metal site structure relaxes within ca. 10 ns to a structure accommodating a higher coordination number than two. Thus, the change from Ag(I) to Cd(II) gives rise to rapid structural change, presumably inactivating the protein's function.

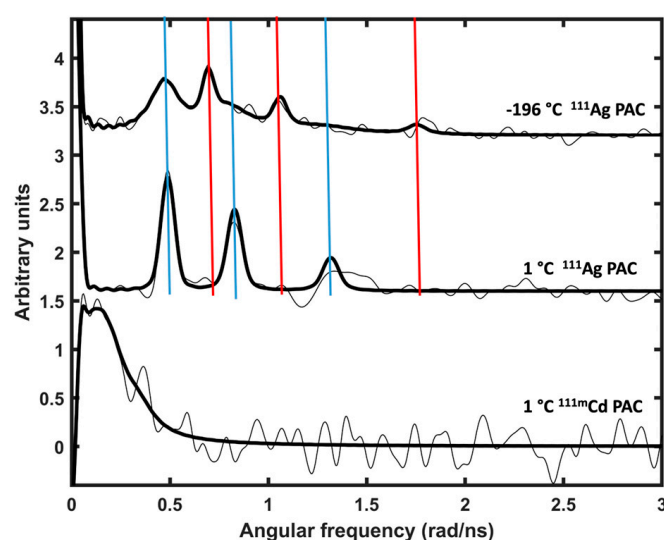


**Figure 7.**  $^{111}\text{Ag}$  and  $^{111\text{m}}\text{Cd}$  PAC spectra recorded for CueR. Two NQIs are present in the top panel, one (NQI1, red) reflecting the native metal site structure (possibly with an additional weak equatorial ligand) and the other (NQI2, blue) reflecting a higher coordination number. NQI2 is exclusively present in the experiment at 1 °C (middle panel), demonstrating that the daughter nucleus, Cd(II), remodels the metal site within ca. 10 ns of  $^{111}\text{Ag}$  decay. The Fourier transform for  $^{111}\text{Ag}$  PAC is multiplied by  $-1$  for easy comparison with the Fourier transform for  $^{111\text{m}}\text{Cd}$  PAC. Reprinted with permission from ref. [32]. Copyright 2020 the authors, published by Wiley-VCH Verlag GmbH & Co.

A  $^{111\text{m}}\text{Cd}$  PAC experiment, see the lower panel of Figure 7, gave a very low-frequency NQI, presumably originating from coordination by four cysteinates, demonstrating that at thermodynamic equilibrium, Cd(II) most likely recruits two additional Cys ligands, which are available in the C-terminal CCHHRAG fragment.

### 3.5. Potential Future Applications

$^{111}\text{Ag}$  PAC spectroscopy has so far not been applied extensively in bioinorganic chemistry, nor in any other field. Here, we briefly present some examples for which  $^{111}\text{Ag}$  could potentially provide useful and unique information.

#### 3.5.1. Cu(I) Binding Sites in Redox Active Proteins

Characterization of the metal site structure of Cu(I) in redox active, copper-dependent proteins is an obvious target for the application of  $^{111}\text{Ag}$  PAC. The simplest case would be enzymes with a single copper site, for example, lytic polysaccharide monooxygenases (LPMOs), amine oxidase, heme-copper oxidase, nitrite reductase, and superoxide dis-

mutase (SOD) if the Ag(I)Zn(II)-SOD species can be prepared. Moreover, mixed species of multicopper proteins with Cu(I/II) and Ag(I) might be characterized, assuming that well-defined species may be prepared with certain sites occupied by copper ion(s) and others by silver ion(s) [11]. In particular, this would allow for elucidation of Cu(I) binding site structures of intermediates in reaction cycles where Ag(I) prevents the oxidation at the site it occupies. Although this may be highly challenging and perhaps impossible for multi-copper sites (type II and type III copper sites), Ag(I) substitution in mononuclear copper sites (type I copper sites) of multicopper oxidases might be achieved.

### 3.5.2. Cu(I) Binding Sites in Cu(I) Transporting ATPases

Cu(I) transport out of cells is accomplished by transmembrane ATP-dependent transporters [44]. The details of Cu(I) coordination at a number of transiently occupied sites within these large proteins might be elucidated by  $^{111}\text{Ag}$  PAC spectroscopy. The opportunity to explore metal ion transporters pertains not only to  $^{111}\text{Ag}$ (I), but also to other PAC isotopes, such as  $^{111\text{m}}\text{Cd}$ (II), which might be applied to explore, e.g., Zn(II) transport. Such studies have not been conducted yet.

### 3.5.3. Methionine Containing Cu(I) Binding Sites

Cu(I) is a relatively soft metal ion, and often displays binding to soft ligands such as sulfur. In the cytosol, cysteine thiolates are commonly found at Cu(I) binding sites of both metallochaperones and metalloregulatory proteins, *vide supra*. However, under more oxidizing conditions, e.g., extracellularly or in the periplasm of prokaryotic organisms, methionine takes part in the coordination of Cu(I), and even so-called methionine-only binding sites have been identified [11,12,45–56]. It is conceivable that  $^{111}\text{Ag}$  PAC spectroscopy can provide further elucidation of the metal site structure and flexibility at such metal sites.

### 3.5.4. Low Temperature Experiments

The decay of  $^{111}\text{Ag}$ (I) to  $^{111}\text{Cd}$ (II) is accompanied by an almost instantaneous change of element and oxidation state, and additionally the Cd daughter nucleus receives a significant amount of recoil kinetic energy (up to around 500 kJ/mol) in a direction depending on the direction of emission of the  $\beta^-$  and the antineutrino. It has been demonstrated by QM/MD simulations [43] that the recoil energy is dissipated to the surrounding protein within picoseconds. The nuclear decay gives a unique opportunity to explore these relaxation processes, and thus probe the protein metal site flexibility/rigidity. However, if the aim is to characterize the Cu(I) metal site structure, the nuclear decay is an undesired complication which can, to some extent, be alleviated by conducting the experiments at low sample temperatures. This is illustrated by the  $^{111}\text{Ag}$  PAC data recorded for the Cu(I)-sensing CueR protein, *vide supra*. Thus, there may be a significant advantage to running experiments at low sample temperatures to elucidate Cu(I) metal site structures, and it seems likely that at even lower temperatures, e.g., using a He cryostat, may further enhance the trapping of the native metal site structure.

**Funding:** LH thanks the Danish Agency for Higher Education and Science for support via the NICE grant, reference number 177363.

**Conflicts of Interest:** The authors declare no conflict of interest.

## References

1. Giedroc, D.P.; Arunkumar, A.I. Metal Sensor Proteins: Nature's Metalloregulated Allosteric Switches. *Dalton Trans.* **2007**, 3107–3120. [[CrossRef](#)]
2. Osman, D.; Cavet, J.S. Chapter 8—Copper Homeostasis in Bacteria. In *Advances in Applied Microbiology*; Laskin, A.I., Sariaslani, S., Gadd, G.M., Eds.; Academic Press: Cambridge, MA, USA, 2008; Volume 65, pp. 217–247; ISBN 0065-2164.
3. Lutsenko, S. Human Copper Homeostasis: A Network of Interconnected Pathways. *Curr. Opin. Chem. Biol.* **2010**, *14*, 211–217. [[CrossRef](#)] [[PubMed](#)]

4. Solomon, E.I.; Heppner, D.E.; Johnston, E.M.; Ginsbach, J.W.; Cirera, J.; Qayyum, M.; Kieber-Emmons, M.; Kjaergaard, C.H.; Hadt, R.G.; Tian, L. Copper Active Sites in Biology. *Chem. Rev.* **2014**, *114*, 3659–3853. [[CrossRef](#)] [[PubMed](#)]
5. Scott, R.A.; Lukehart, C.M. *Applications of Physical Methods to Inorganic and Bioinorganic Chemistry*; John Wiley & Sons Ltd.: Hoboken, NJ, USA, 2007.
6. Jancso, A.; Correia, J.G.; Gottberg, A.; Schell, J.; Stachura, M.; Szunyogh, D.; Pallada, S.; Lupascu, D.C.; Kowalska, M.; Hemmingsen, L. TDPAC and  $\beta$ -NMR Applications in Chemistry and Biochemistry. *J. Phys. G Nucl. Part. Phys.* **2017**, *44*, 064003. [[CrossRef](#)]
7. Summers, M.F.  $^{113}\text{Cd}$  NMR Spectroscopy of Coordination Compounds and Proteins. *Coord. Chem. Rev.* **1988**, *86*, 43–134. [[CrossRef](#)]
8. Bertini, I.; Luchinat, C. The Reaction Pathways of Zinc Enzymes and Related Biological Catalysts. In *Bioinorganic Chemistry*; University Science Books: Mill Valley, CA, USA, 1994; p. 37.
9. Hay, M.T.; Milberg, R.M.; Lu, Y. Preparation and Characterization of Mercury and Silver Derivatives of an Engineered Purple Copper Center in Azurin. *J. Am. Chem. Soc.* **1996**, *118*, 11976–11977. [[CrossRef](#)]
10. Santagostini, L.; Gullotti, M.; Hazzard, J.T.; Maritano, S.; Tollin, G.; Marchesini, A. Inhibition of Intramolecular Electron Transfer in Ascorbate Oxidase by  $\text{Ag}^+$ : Redox State Dependent Binding. *J. Inorg. Biochem.* **2005**, *99*, 600–605. [[CrossRef](#)]
11. Djoko, K.Y.; Chong, L.X.; Wedd, A.G.; Xiao, Z. Reaction Mechanisms of the Multicopper Oxidase CueO from *Escherichia Coli* Support Its Functional Role as a Cuprous Oxidase. *J. Am. Chem. Soc.* **2010**, *132*, 2005–2015. [[CrossRef](#)]
12. Singh, S.K.; Roberts, S.A.; McDevitt, S.F.; Weichsel, A.; Wildner, G.F.; Grass, G.B.; Rensing, C.; Montfort, W.R. Crystal Structures of Multicopper Oxidase CueO Bound to Copper(I) and Silver(I): Functional Role of a Methionine-Rich Sequence. *J. Biol. Chem.* **2011**, *286*, 37849–37857. [[CrossRef](#)]
13. Wilcoxon, J.; Snider, S.; Hille, R. Substitution of Silver for Copper in the Binuclear Mo/Cu Center of Carbon Monoxide Dehydrogenase from *Oligotropha carboxidovorans*. *J. Am. Chem. Soc.* **2011**, *133*, 12934–12936. [[CrossRef](#)]
14. Chauhan, S.; Kline, C.D.; Mayfield, M.; Blackburn, N.J. Binding of Copper and Silver to Single-Site Variants of Peptidylglycine Monooxygenase Reveals the Structure and Chemistry of the Individual Metal Centers. *Biochemistry* **2014**, *53*, 1069–1080. [[CrossRef](#)] [[PubMed](#)]
15. Puchkova, L.V.; Brogini, M.; Polishchuk, E.V.; Ilyechova, E.Y.; Polishchuk, R.S. Silver Ions as a Tool for Understanding Different Aspects of Copper Metabolism. *Nutrients* **2019**, *11*, 1364. [[CrossRef](#)] [[PubMed](#)]
16. Nardella, M.I.; Fortino, M.; Barbanente, A.; Natile, G.; Pietropaolo, A.; Arnesano, F. Multinuclear Metal-Binding Ability of the N-Terminal Region of Human Copper Transporter Ctr1: Dependence Upon pH and Metal Oxidation State. *Front. Mol. Biosci.* **2022**, *9*, 897621. [[CrossRef](#)] [[PubMed](#)]
17. Kircheva, N.; Angelova, S.; Dobrev, S.; Petkova, V.; Nikolova, V.; Dudev, T.  $\text{Cu}^+/\text{Ag}^+$  Competition in Type I Copper Proteins (T1Cu). *Biomolecules* **2023**, *13*, 681. [[CrossRef](#)] [[PubMed](#)]
18. Hemmingsen, L.; Sas, K.N.; Danielsen, E. Biological Applications of Perturbed Angular Correlations of  $\gamma$ -Ray Spectroscopy. *Chem. Rev.* **2004**, *104*, 4027–4062. [[CrossRef](#)] [[PubMed](#)]
19. Tröger, W. Nuclear Probes in Life Sciences. *Hyperfine Interact.* **1999**, *120*, 117–128. [[CrossRef](#)]
20. Tosato, M.; Asti, M.; Di Marco, V.; Jensen, M.L.; Schell, J.; Dang, T.T.; Köster, U.; Jensen, M.; Hemmingsen, L. Towards in Vivo Applications of  $^{111}\text{Ag}$  Perturbed Angular Correlation of  $\gamma$ -Rays (PAC) Spectroscopy. *Appl. Radiat. Isot.* **2022**, *190*, 110508. [[CrossRef](#)]
21. Haas, H.; Shirley, D.A. Nuclear Quadrupole Interaction Studies by Perturbed Angular Correlations. *J. Chem. Phys.* **1973**, *58*, 3339–3355. [[CrossRef](#)]
22. Lerf, A.; Butz, T. Nuclear Quadrupole Interactions in Compounds Studied by Time Differential Perturbed Angular Correlations/Distributions. *Hyperfine Interact.* **1987**, *36*, 275–370. [[CrossRef](#)]
23. Hansen, B.; Bukrinsky, J.T.; Hemmingsen, L.; Bjerrum, M.J.; Singh, K.; Bauer, R. Effects of the Nuclear Transformation  $^{111}\text{Ag}(\text{I})$  to  $^{111}\text{Cd}(\text{II})$  in a Single Crystal of  $\text{Ag}[^{111}\text{Ag}](\text{Imidazole})_2\text{NO}_3$ . *Phys. Rev. B* **1999**, *59*, 14182–14190. [[CrossRef](#)]
24. Haas, H.; Röder, J.; Correia, J.G.; Schell, J.; Fenta, A.S.; Vianden, R.; Larsen, E.M.H.; Aggelund, P.A.; Fromsejer, R.; Hemmingsen, L.B.S.; et al. Free Molecule Studies by Perturbed  $\gamma$ - $\gamma$  Angular Correlation: A New Path to Accurate Nuclear Quadrupole Moments. *Phys. Rev. Lett.* **2021**, *126*, 103001. [[CrossRef](#)] [[PubMed](#)]
25. Mauk, M.R.; Gamble, R.C.; Baldeschwieler, J.D. Vesicle Targeting: Timed Release and Specificity for Leukocytes in Mice by Subcutaneous Injection. *Science* **1980**, *207*, 309–311. [[CrossRef](#)] [[PubMed](#)]
26. Bauer, R.; Danielsen, E.; Hemmingsen, L.; Bjerrum, M.J.; Hansson, O.; Singh, K. Interplay between Oxidation State and Coordination Geometry of Metal Ions in Azurin. *J. Am. Chem. Soc.* **1997**, *119*, 157–162. [[CrossRef](#)]
27. Danielsen, E.; Kroes, S.J.; Canters, G.W.; Bauer, R.; Hemmingsen, L.; Singh, K.; Messerschmidt, A. Coordination Geometries for Monovalent and Divalent Metal Ions in [His121] Azurin. *Eur. J. Biochem.* **1997**, *250*, 249–259. [[CrossRef](#)] [[PubMed](#)]
28. Danielsen, E.; Scheller, H.V.; Bauer, R.; Hemmingsen, L.; Bjerrum, M.J.; Hansson, O. Plastocyanin Binding to Photosystem I as a Function of the Charge State of the Metal Ion: Effect of Metal Site Conformation. *Biochemistry* **1999**, *38*, 11531–11540. [[CrossRef](#)] [[PubMed](#)]
29. Sas, K.N.; Haldrup, A.; Hemmingsen, L.; Danielsen, E.; Øgdenal, L.H. pH-Dependent Structural Change of Reduced Spinach Plastocyanin Studied by Perturbed Angular Correlation of  $\gamma$ -Rays and Dynamic Light Scattering. *J. Biol. Inorg. Chem.* **2006**, *11*, 409–418. [[CrossRef](#)] [[PubMed](#)]

30. Holm, J.K.; Hemmingsen, L.; Bubacco, L.; Salvato, B.; Bauer, R. Interaction and Coordination Geometries for Ag(I) in the Two Metal Sites of Hemocyanin. *Eur. J. Biochem.* **2000**, *267*, 1754–1760. [CrossRef]
31. Liu, T.; Chen, X.; Ma, Z.; Shokes, J.; Hemmingsen, L.; Scott, R.A.; Giedroc, D.P. A Cu<sup>I</sup>-Sensing ArsR Family Metal Sensor Protein with a Relaxed Metal Selectivity Profile. *Biochemistry* **2008**, *47*, 10564–10575. [CrossRef]
32. Balogh, R.K.; Gyurcsik, B.; Jensen, M.; Thulstrup, P.W.; Köster, U.; Christensen, N.J.; Mørch, F.J.; Jensen, M.L.; Jancsó, A.; Hemmingsen, L. Flexibility of the CueR Metal Site Probed by Instantaneous Change of Element and Oxidation State from Ag<sup>I</sup> to Cd<sup>II</sup>. *Chem. Eur. J.* **2020**, *26*, 7451–7457. [CrossRef]
33. Balogh, R.K.; Gyurcsik, B.; Jensen, M.; Thulstrup, P.W.; Köster, U.; Christensen, N.J.; Jensen, M.L.; Hunyadi-Gulyás, E.; Hemmingsen, L.; Jancsó, A. Tying Up a Loose End: On the Role of the C-Terminal CCHHRAG Fragment of the Metalloregulator CueR. *ChemBioChem* **2022**, *23*, e202200290. [CrossRef]
34. Shepard, W.E.B.; Anderson, B.F.; Lewandoski, D.A.; Norris, G.E.; Baker, E.N. Copper Coordination Geometry in Azurin Undergoes Minimal Change on Reduction of Copper(II) to Copper(I). *J. Am. Chem. Soc.* **1990**, *112*, 7817–7819. [CrossRef]
35. Guss, J.M.; Bartunik, H.D.; Freeman, H.C. Accuracy and Precision in Protein Structure Analysis: Restrained Least-Squares Refinement of the Structure of Poplar Plastocyanin at 1.33 Å Resolution. *Acta Crystallogr. Sect. B Struct. Sci.* **1992**, *48*, 790–811. [CrossRef]
36. Shepard, W.E.B.; Kingston, R.L.; Anderson, B.F.; Baker, E.N. Structure of Apo-Azurin from *Alcaligenes Denitrificans* at 1.8 Å Resolution. *Acta Crystallogr. Sect. D Biol. Crystallogr.* **1993**, *49*, 331–343. [CrossRef] [PubMed]
37. LLC The PyMOL Molecular Graphics System, Version 2.5.5; Schrödinger: New York, NY, USA, 2015. Available online: <https://pymol.org/2/support.html?> (accessed on 25 August 2023).
38. Guss, J.M.; Harrowell, P.R.; Murata, M.; Norris, V.A.; Freeman, H.C. Crystal Structure Analyses of Reduced (Cu<sup>I</sup>) Poplar Plastocyanin at Six pH Values. *J. Mol. Biol.* **1986**, *192*, 361–387. [CrossRef] [PubMed]
39. Hazes, B.; Kalk, K.H.; Hol, W.G.J.; Magnus, K.A.; Bonaventura, C.; Bonaventura, J.; Dauter, Z. Crystal Structure of Deoxygenated *Limulus Polyphemus* Subunit II Hemocyanin at 2.18 Å Resolution: Clues for a Mechanism for Allosteric Regulation. *Protein Sci.* **1993**, *2*, 597–619. [CrossRef] [PubMed]
40. Bauer, R.; Jensen, S.J.; Schmidt-Nielsen, B. The Angular Overlap Model Applied to the Calculation of Nuclear Quadrupole Interactions. *Hyperfine Interact.* **1988**, *39*, 203–234. [CrossRef]
41. Changela, A.; Chen, K.; Xue, Y.; Holschen, J.; Outten, C.E.; O'Halloran, T.V.; Mondragón, A. Molecular Basis of Metal-Ion Selectivity and Zeptomolar Sensitivity by CueR. *Science* **2003**, *301*, 1383–1387. [CrossRef]
42. Philips, S.J.; Canalizo-Hernandez, M.; Yildirim, I.; Schatz, G.C.; Mondragón, A.; O'Halloran, T.V. Allosteric Transcriptional Regulation via Changes in the Overall Topology of the Core Promoter. *Science* **2015**, *349*, 877–881. [CrossRef]
43. Fromsejer, R.; Mikkelsen, K.V.; Hemmingsen, L. Dynamics of Nuclear Recoil: QM-BOMD Simulations of Model Systems Following  $\beta$ -Decay. *Phys. Chem. Chem. Phys.* **2021**, *23*, 25689–25698. [CrossRef]
44. Gourdon, P.; Liu, X.-Y.; Skjørringe, T.; Morth, J.P.; Møller, L.B.; Pedersen, B.P.; Nissen, P. Crystal Structure of a Copper-Transporting PIB-Type ATPase. *Nature* **2011**, *475*, 59–64. [CrossRef]
45. Peariso, K.; Huffman, D.L.; Penner-Hahn, J.E.; O'Halloran, T.V. The PcoC Copper Resistance Protein Coordinates Cu(I) via Novel S-Methionine Interactions. *J. Am. Chem. Soc.* **2003**, *125*, 342–343. [CrossRef]
46. Wernimont, A.K.; Huffman, D.L.; Finney, L.A.; Demeler, B.; O'Halloran, T.V.; Rosenzweig, A.C. Crystal Structure and Dimerization Equilibria of PcoC, a Methionine-Rich Copper Resistance Protein from *Escherichia coli*. *J. Biol. Inorg. Chem.* **2003**, *8*, 185–194. [CrossRef] [PubMed]
47. Arnesano, F.; Banci, L.; Bertini, I.; Mangani, S.; Thompsett, A.R. A Redox Switch in CopC: An Intriguing Copper Trafficking Protein That Binds Copper(I) and Copper(II) at Different Sites. *Proc. Natl. Acad. Sci. USA* **2003**, *100*, 3814–3819. [CrossRef] [PubMed]
48. Banci, L.; Bertini, I.; Ciofi-Baffoni, S.; Katsari, E.; Katsaros, N.; Kubicek, K.; Mangani, S. A Copper(I) Protein Possibly Involved in the Assembly of CuA Center of Bacterial Cytochrome c Oxidase. *Proc. Natl. Acad. Sci. USA* **2005**, *102*, 3994–3999. [CrossRef] [PubMed]
49. Jiang, J.; Nadas, I.A.; Kim, M.A.; Franz, K.J. A Mets Motif Peptide Found in Copper Transport Proteins Selectively Binds Cu(I) with Methionine-Only Coordination. *Inorg. Chem.* **2005**, *44*, 9787–9794. [CrossRef]
50. Zhang, L.; Koay, M.; Maher, M.J.; Xiao, Z.; Wedd, A.G. Intermolecular Transfer of Copper Ions from the CopC Protein of *Pseudomonas Syringae*. Crystal Structures of Fully Loaded Cu<sup>I</sup>Cu<sup>II</sup> Forms. *J. Am. Chem. Soc.* **2006**, *128*, 5834–5850. [CrossRef]
51. Bagai, I.; Liu, W.; Rensing, C.; Blackburn, N.J.; McEvoy, M.M. Substrate-Linked Conformational Change in the Periplasmic Component of a Cu(I)/Ag(I) Efflux System. *J. Biol. Chem.* **2007**, *282*, 35695–35702. [CrossRef]
52. Xue, Y.; Davis, A.V.; Balakrishnan, G.; Stasser, J.P.; Staehlin, B.M.; Focia, P.; Spiro, T.G.; Penner-Hahn, J.E.; O'Halloran, T.V. Cu(I) Recognition via Cation- $\pi$  and Methionine Interactions in CusF. *Nat. Chem. Biol.* **2008**, *4*, 107–109. [CrossRef]
53. Davis, A.V.; O'Halloran, T.V. A Place for Thioether Chemistry in Cellular Copper Ion Recognition and Trafficking. *Nat. Chem. Biol.* **2008**, *4*, 148–151. [CrossRef]
54. Rubino, J.T.; Riggs-Gelasco, P.; Franz, K.J. Methionine Motifs of Copper Transport Proteins Provide General and Flexible Thioether-Only Binding Sites for Cu(I) and Ag(I). *J. Biol. Inorg. Chem.* **2010**, *15*, 1033–1049. [CrossRef]

55. Miranda-Blancas, R.; Avelar, M.; Rodriguez-Arteaga, A.; Sinicropi, A.; Rudiño-Piñera, E. The  $\beta$ -Hairpin from the *Thermus thermophilus* HB27 Laccase Works as a PH-Dependent Switch to Regulate Laccase Activity. *J. Struct. Biol.* **2021**, *213*, 107740. [[CrossRef](#)] [[PubMed](#)]
56. Roulling, F.; Godin, A.; Feller, G. Function and Versatile Location of Met-Rich Inserts in Blue Oxidases Involved in Bacterial Copper Resistance. *Biochimie* **2022**, *194*, 118–126. [[CrossRef](#)] [[PubMed](#)]

**Disclaimer/Publisher's Note:** The statements, opinions and data contained in all publications are solely those of the individual author(s) and contributor(s) and not of MDPI and/or the editor(s). MDPI and/or the editor(s) disclaim responsibility for any injury to people or property resulting from any ideas, methods, instructions or products referred to in the content.